An Analytical and Experimental Study of Impulsive Stress of Square Plates at an Impact Loading Point by the 3-Dimensional Dynamic Theory of Elasticity

Kwang-Hee Im,* Kim Sun-Kyu and In-Young Yang*****

(Received January 3, 1994)

In this paper, a new method is proposed to analyze impulsive stresses at an impact loading point, which cannot be solved by the classical plate theory. Particularly, impulsive stresses at an impact loading point under any impact conditions(regardless of mass of impactor, velocity of impactor, stiffness of plate, etc.), can be obtained by the three-dimensional dynamic theory of elasticity and potential theory of displacement.

In addition, by using the Hertzian contact theory, impact loading can be analyzed to account for the local deformation, and this load is applied to the impulsive stress analysis by approximating the impact loading to an analyzable function. In the numerical analysis, the fast Fourier transform(FFT) algorithm and the numerical inverse Laplace transformation are utilized.

Using a new equation, it was possible to analyze impulsive stresses at an impact loading point, and good agreement between the experimental and theoretical results was established.

Key Words: Hertzian Contact Theory, Impulsive Stresses, Stress Function, Three-Dimensional Dynamic Theory of Elasticity, Functional Equation of Impact Loading

1. Introduction

When a machine or structual component is subjected to impact loading, unexpected dynamic behavior occurs under the static loading, causing unexpected failure and deformation of materials because of stress wave effects.

To prove the dynamic phenomena generating in the materials, research activities have recently been made on impact problems(Wang and Yew, 1989; Holian, 1990) of plates by high-speed shooting of the impactor, and on the impact problems of structual members(Kishimoto, Aoki and Sakata, 1980).

Clearly, impact strength must be analyzed on impact problems of plates, which are widely used for the structual plate members, and displacement can possibly be analyzed at a point of concentrated impact loading by classical plate theory using the analyses of impulsive responses on plates ; but currently, impulsive stresses could not be analyzed because of failure of convergence of Solutions at the point of concentrated impact loading(Timoshenko and Winowsky, 1959; Ugural, 1981).

Recently, to analyze impulsive stresses at the concentrated impact loading point, Ujihashi(1983) analyzed the impulsive stresses by using the high-order approximate theory, but there is a difference between analytical and experimental results. Also, Ujihashi, etc.(Ujihashi, Adachi, Inoue and Matsumoto, 1986) and Yang(1988) analyzed implusive stresses at a concentrated

*Graduate Student, Department of Mechanical Engineering, Chosun University

**Department of Automobile Engineering,Iri Nat'l College of Agriculture and Technology, Iri, Chollabukdo 570-110, Korea

***Department of Mechanical Design Engineering, Chosun University 375 Susuk-Dong, Dong-Gu Kwangju 501-759, Korea

impact loading point by the three-dimensional dynamic theory of elasticty, only in the case of light impactor, relatively high collision velocity and thick plate. Especially, solutions of these analytical results are overestimated for practical phenomena and the analytical range of implusive stress has a definite domain. Therefore, these analytical methods cannot be applied to wide impact range.

Thus, in this study, regardless of dimensions of impact load coefficeient considering density of plate, collision velocity, dimension of plate stiffness and size of impactor, a new functional approximation equation of impact loading was presented to analyze the impulsive stresses at an impact loading point under any impact conditions.

When the measurement of impact loading is difficult, the impact loading is obtained by using the Lagrange's classical theory and Hertz's contact theory which consider local deformation by collision of steel ball and plate. The impact loading obtained above is made into an analyzable function for an approximate equation. The stress function and three-dimensional dynamic theory of elasticity are introduced. To give credit to this analytical method, the results of measured strain are compared with numerically calculated solutions of analytical method presented in this study, and the former agree well with the calculated solutions.

2. Theoretical Analysis

2.1 Stress analysis

In the case where the center zone of a square plate($2c \times 2c$) simply supported at four edges is subjected to partially distributed impact loading $q_o f(t)$ as shown in Fig. 1, impulsive stresses generated at the square plate are to be analyzed(Yang, 1988). Let orthogonal coordinates(x, y, z) denote u, v, w of displacement components, σ_x, σ_y, σ_z of normal stress components and τ_{xy}, τ_{xz}, τ_{yz} of shear strain components at the center point of the square plate($2c \times 2c$). The three-dimensional dynamic theory of elasticity is defined as follows (Johnson, 1972):

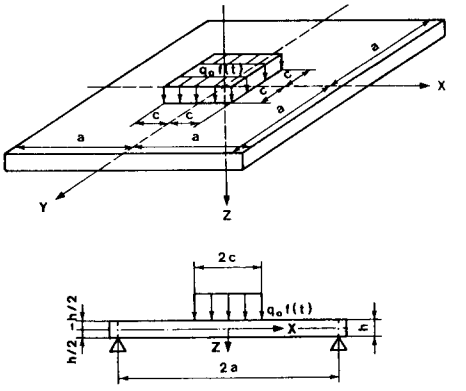

Fig. 1 A square plate subjected to partially distributed impact loading on center($2c \times 2c$)

$$\frac{\partial \sigma_x}{\partial x}+\frac{\partial \tau_{yx}}{\partial y}+\frac{\partial \tau_{zx}}{\partial z}=\rho\frac{\partial^2 u}{\partial t^2}$$
$$\frac{\partial \tau_{xy}}{\partial x}+\frac{\partial \sigma_y}{\partial y}+\frac{\partial \tau_{zy}}{\partial z}=\rho\frac{\partial^2 v}{\partial t^2}$$
$$\frac{\partial \tau_{xz}}{\partial x}+\frac{\partial \tau_{yz}}{\partial y}+\frac{\partial \sigma_z}{\partial z}=\rho\frac{\partial^2 w}{\partial t^2} \tag{1}$$

Substitution from the relation equations for stress-strain and strain-displacement into Eq. (1) leads to displacement Eq. (2) as follows(Ni, 1985):

$$\nabla^2 u+\frac{1}{1-2\nu}\frac{\partial e}{\partial x}=\frac{\rho}{G}\frac{\partial^2 u}{\partial t^2}$$
$$\nabla^2 v+\frac{1}{1-2\nu}\frac{\partial e}{\partial y}=\frac{\rho}{G}\frac{\partial^2 v}{\partial t^2}$$
$$\nabla^2 w+\frac{1}{1-2\nu}\frac{\partial e}{\partial z}=\frac{\rho}{G}\frac{\partial^2 w}{\partial t^2}$$
$$e=\frac{\partial u}{\partial x}+\frac{\partial v}{\partial y}+\frac{\partial w}{\partial z} \tag{2}$$

where G is the shear elastic modulus.

The displacement components can be obtained by introducing displacement potential(φ_o, λ_1, λ_2, λ_3) theory(Nakahara, 1977; Achenbach, 1975) to solve the displacement Eq. (2) as follows:

$$2Gu=\frac{\partial \varphi_o}{\partial x}+\frac{\partial \lambda_3}{\partial y}-\frac{\partial \lambda_2}{\partial z}$$
$$2Gv=\frac{\partial \varphi_o}{\partial y}+\frac{\partial \lambda_3}{\partial z}-\frac{\partial \lambda_2}{\partial x}$$
$$2Gw=\frac{\partial \varphi_o}{\partial z}+\frac{\partial \lambda_3}{\partial x}-\frac{\partial \lambda_2}{\partial y} \tag{3}$$

To obtain displacement compontents, the solutions of displacement potential can be approximately given by:

$$\varphi_o=\Phi_{mn}\cos\alpha_m x\cos\alpha_n y,$$
$$\lambda_1=\Delta^1_{mn}\cos\alpha_m x\sin\alpha_n y$$
$$\lambda_2=\Delta^2_{mn}\sin\alpha_m x\cos\alpha_n y,$$
$$\lambda_3=\Delta^3_{mn}\sin\alpha_m x\sin\alpha_n y \tag{4}$$

where $\alpha_m=\dfrac{\pi(2m-1)}{2a}$, $\alpha_n=\dfrac{\pi(2n-1)}{2a}$

$(m,\ n=1,\ 2,\ \cdots)$

and Φ_{mn}, Δ^1_{mn}, Δ^2_{mn}, Δ^3_{mn} are the functions having two undetermined coefficients at the general solutions.

Here, in the absence of the Z-directional rotation, $\lambda_3=0$.

Substitution of Eq. (3) into Eq. (2) yields the governing wave equations as.

$$\nabla^2\varphi_o=\frac{1}{c_1^2}\frac{\partial^2\phi_o}{\partial t^2},\quad \nabla^2\lambda_1=\frac{1}{c_2^2}\frac{\partial^2\lambda_1}{\partial t^2},$$
$$\nabla^2\lambda_2=\frac{1}{c_2^2}\frac{\partial^2\lambda_2}{\partial t^2} \tag{5}$$

where $c_1^2=\dfrac{2(1-\nu)}{1-2\nu}\dfrac{G}{\rho}$, $c_2^2=\dfrac{G}{\rho}$

ν is the Poisson's ratio of plate, ρ is the mass density of plate, c_1 is the propagation velocity of longitudinal wave, and c_2 is the propagation velocity of shear wave.

The use of stress-strain and strain displacement relation in Eq. (3) came up to the relation-equations of stress components and displacement potential as follows:

$$\sigma_x=\frac{\partial^2\varphi_o}{\partial x^2}-\frac{\partial^2\lambda_2}{\partial x\partial z}+\frac{\nu}{1-2\nu}\nabla^2\varphi_o$$
$$\sigma_y=\frac{\partial^2\varphi_o}{\partial y^2}-\frac{\partial^2\lambda_1}{\partial y\partial z}+\frac{\nu}{1-2\nu}\nabla^2\varphi_o$$
$$\sigma_z=\frac{\partial^2\varphi_o}{\partial z^2}+\frac{\partial^2\lambda_2}{\partial x\partial z}-\frac{\partial^2\lambda_1}{\partial z\partial y}+\frac{\nu}{1-2\nu}\nabla^2\varphi_o$$
$$\tau_{xy}=\frac{\partial^2\varphi_o}{\partial x\partial y}+\frac{1}{2}\left(\frac{\partial^2\lambda_1}{\partial x\partial z}-\frac{\partial^2\lambda_2}{\partial y\partial z}\right)$$
$$\tau_{xz}=\frac{\partial^2\varphi_o}{\partial x\partial z}+\frac{1}{2}\left(\frac{\partial^2\lambda_2}{\partial x^2}-\frac{\partial^2\lambda_1}{\partial x\partial y}-\frac{\partial^2\lambda_2}{\partial z^2}\right)$$
$$\tau_{yz}=\frac{\partial^2\varphi_o}{\partial z\partial y}+\frac{1}{2}\left(\frac{\partial^2\lambda_2}{\partial x\partial y}-\frac{\partial^2\lambda_1}{\partial y^2}-\frac{\partial^2\lambda_1}{\partial z^2}\right) \tag{6}$$

Because Eq. (5) are differential equations of the second order on coordinates$(x,\ y,\ z)$ and time(t), the ordinary differentional equations of x, y, z can be obtained by applying the Laplace transformation to them.

The initial conditions of displacement potential on a square plate before impact$(t\leq 0)$ can be expressed as:

$$(u,\ v,\ w)_{t=o}=0,$$
$$\left(\frac{\partial u}{\partial t},\ \frac{\partial v}{\partial t},\ \frac{\partial w}{\partial t}\right)_{t=o}=0 \tag{7}$$

Equation (8) can be obtained by the Laplace transformation(Eq. (5)) as follows:

$$\nabla^2\bar{\varphi}_o=\frac{p^2}{c_1^2}\bar{\varphi}_o,\ \cdots\ \nabla^2\bar{\lambda}_1=\frac{p^2}{c_2^2}\bar{\lambda}_1,$$
$$\nabla^2\bar{\lambda}_2=\frac{p^2}{c_2^2}\bar{\lambda}_2 \tag{8}$$

where $\bar{\varphi}_o=\int_0^\infty\varphi_o e^{-pt}dt$, $\bar{\lambda}_1=\int_0^\infty\lambda_1 e^{-pt}dt$, $\bar{\lambda}_2=\int_0^\infty\lambda_2 e^{-pt}dt$

and p is the parameter of Laplace.

Substitution of Eq. (5) into (8) leads to the following ordinary differentional equations:

$$\frac{d^2\bar{\Phi}_{mn}}{dz^2}=\left(\alpha_m^2+\alpha_n^2+\frac{p^2}{c_1^2}\right)\bar{\Phi}_{mn}$$
$$\frac{d^2\bar{\Delta}^1_{mn}}{dz^2}=\left(\alpha_m^2+\alpha_n^2+\frac{p^2}{c_2^2}\right)\bar{\Delta}^1_{mn}$$
$$\frac{d^2\bar{\Delta}^2_{mn}}{dz^2}=\left(\alpha_m^2+\alpha_n^2+\frac{p^2}{c_2^2}\right)\bar{\Delta}^2_{mn} \tag{9}$$

Where general solutions of Eq. (9) can be defined as:

$$\bar{\varphi}_o=\sum_{m=1}^{\infty}\sum_{n=1}^{\infty}[C_1\exp(\beta_{mnz})+C_2\exp(-\beta_{mnz})]\cos\alpha_m x\cos\alpha_n y$$
$$\bar{\lambda}_1=\sum_{m=1}^{\infty}\sum_{n=1}^{\infty}[D_1\exp(\gamma_{mnz})+D_2\exp(-\gamma_{mnz})]\cos\alpha_m x\sin\alpha_n y$$
$$\bar{\lambda}_2=\sum_{m=1}^{\infty}\sum_{n=1}^{\infty}[E_1\exp(\gamma_{mnz})+E_2\exp(-\gamma_{mnz})]\sin\alpha_m x\cos\alpha_n y \tag{10}$$

Here,

$$\beta_{mn}^2=\left(\alpha_m^2+\alpha_n^2+\frac{p^2}{c_1^2}\right),\ \gamma_{mn}^2=\left(\alpha_m^2+\alpha_n^2+\frac{p^2}{c_2^2}\right)$$

and C_1, C_2, D_1, D_2, E_1, E_2 are unknown coefficients to be determined by boundary conditions. The boundary conditions can be expressed as follows: (See Fig. 1)

(i) $\tau_{zx}=\tau_{zy}=0$ at $Z=-h/2$
(upper side of plate)
$\sigma_z=-q_o f(t)U(c-|x|)U(c-|y|)$

(ii) $\sigma_z=\tau_{zx}=\tau_{zy}=0$ at $Z=h/2$
(lower side of plate) (11)

where $U(c-|x|)\times U(c-|y|)$ denotes the unit step function.

The Laplace transformation of the Eq. (11) becomes

$$\begin{aligned}&(\text{i})\ \hat{\sigma}_z=-q_o\hat{f}(p)H(c-|x|)H(c-|y|),\\&\quad\hat{\tau}_{xz}=\tau_{zy}=0 \text{ at } Z=-h/2\\&(\text{ii})\ \hat{\sigma}_z=\hat{\tau}_{xz}=\hat{\tau}_{zy}=0 \text{ at } Z=h/2\end{aligned}\quad(12)$$

where $\hat{f}(p)=\int_0^\infty f(t)e^{-pt}dt$

After substituting the general Eq. (10) into the Eq. (6) and the boundary condition Eq. (12) into the Eq. (6), we can find the unknown coefficients(C_1, C_2, D_1, D_2, E_1, E_2).

However, in the expression for $\hat{\sigma}_z$ the right hand side term denotes a periodic function and the left term means a unit step function. Therefor Fourier cosine transformation can utilized and the result is as follows:

$$\begin{aligned}\hat{\sigma}_z=&\sum_{m=1}^{\infty}\sum_{n=1}^{\infty}[\beta_{mn}^2\exp\left(-\frac{\beta_{mnz}}{2}\right)C_1\\&+\beta_{mn}^2\exp\left(\frac{\beta_{mnz}}{2}\right)C_2\\&-\alpha_n\beta_{mn}\exp(-\beta_{mnz}/2)D_1\\&+\alpha_n\beta_{mn}\exp(-\beta_{mnz}/2)D_2\\&+\beta_{mn}\alpha_m\exp(-\beta_{mnz}/2)E_1\\&-\beta_{mn}\alpha_m\exp(\beta_{mnz}/2)E_2]\\=&-q_o\hat{f}(t)\frac{4\sin(\alpha_mc)\sin(\alpha_nc)}{\alpha_m\alpha_na^2}\end{aligned}\quad(13)$$

The acting area($2c$) of partially distributed loading can converge into zero by making the right hand side term of Eq. (13) to be a concentrated loading. Considering the concentrated load(F_o) acting on the plate(Yang, 1988), the following can be written:

$$\begin{aligned}&\lim_{c\to0}4q_oC^2\frac{\sin(\alpha_mC)\sin(\alpha_nC)}{a^2(\alpha_mC)(\alpha_nC)}=\frac{F_o}{a^2}\\&F_o=4C^2q_o\end{aligned}\quad(14)$$

By obtaining a simultaneous equations of the sixth degree by using the foregoing equation, one can determine the unknown coefficients(C_1, C_2, D_1, D_2, E_1, E_2). After this, substituting these equations into Eq. (10) leads to stress-component equations as follows:

$$\begin{aligned}\hat{\sigma}_x=&\sum_{m=1}^{\infty}\sum_{n=1}^{\infty}[(-\alpha_m^2+\frac{\nu P^2}{(1-2\nu)c_1^2})\exp(\beta_{mnz})C_1\\&+(-\alpha_m^2+\frac{\nu P^2}{(1-2\nu)c_1^2})\exp(\beta_{mnz})C_2\\&-\alpha_m\gamma_{mn}\exp(\gamma_{mnz})E_1\\&+\alpha_m\gamma_{mn}\exp(-\gamma_{mnz})E_2]\cos\alpha_mx\cos\alpha_ny\\\hat{\sigma}_y=&\sum_{m=1}^{\infty}\sum_{n=1}^{\infty}[(-\alpha_n^2+\frac{\nu P^2}{(1-2\nu)c_1^2})\exp(\beta_{mnz})C_1\\&+(-\alpha_n^2+\frac{\nu P^2}{(1-2\nu)c_1^2})\exp(-\beta_{mnz})C_2\\&+\alpha_n\gamma_{mn}\exp(\gamma_{mnz})D_1\\&+\alpha_n\gamma_{mn}\exp(-\gamma_{mnz})D_2]\cos\alpha_mx\cos\alpha_ny\\\hat{\sigma}_z=&\sum_{m=1}^{\infty}\sum_{n=1}^{\infty}[(\beta_{mn}^2+\frac{\nu P^2}{(1-2\nu)c_1^2})\exp(\beta_{mnz})C_1\\&+(\beta_{mn}^2+\frac{\nu P^2}{(1-2\nu)c_1^2})\exp(-\beta_{mnz})C_2\\&-\gamma_{mn}\alpha_n\exp(\gamma_{mnz})D_1\\&+\alpha_m\gamma_{mn}\exp(-\gamma_{mnz})D_2\\&+\alpha_m\gamma_{mn}\exp(\gamma_{mnz})E_1\\&-\alpha_m\gamma_{mn}\exp(-\gamma_{mnz})E_2]\cos\alpha_mx\cos\alpha_ny\end{aligned}\quad(15)$$

Additionally, strain-component equations can be expressed as follows:

$$\begin{aligned}\hat{\varepsilon}_x=&\sum_{m=1}^{\infty}\sum_{n=1}^{\infty}\frac{1}{2G}[(-\alpha_m^2)\{C_1\exp(\beta_{mnz})\\&+C_2\exp(-\beta_{mnz})\}\\&-\alpha_m\gamma_{mn}\{E_1\exp(\gamma_{mnz})\\&-E_2\exp(-\gamma_{mnz})\}]\cos\alpha_mx\cos\alpha_ny\\\hat{\varepsilon}_y=&\sum_{m=1}^{\infty}\sum_{n=1}^{\infty}\frac{1}{2G}[(-\alpha_n^2)\{C_1\exp(\beta_{mnz})\\&+C_2\exp(-\beta_{mnz})\}\\&+\alpha_n\gamma_{mn}\{E_1\exp(\gamma_{mnz})\\&-D_2\exp(-\gamma_{mnz})\}]\cos\alpha_mx\cos\alpha_ny\\\hat{\varepsilon}_z=&\sum_{m=1}^{\infty}\sum_{n=1}^{\infty}\frac{1}{2G}[(\beta_{mn}^2)\{C_1\exp(\beta_{mnz})\\&+C_2\exp(-\beta_{mnz})\}\\&+\alpha_m\gamma_{mn}\{E_1\exp(\gamma_{mnz})\\&-E_2\exp(-\gamma_{mnz})\}\\&-\alpha_n\gamma_{mn}\{D_1\exp(\gamma_{mnz})\\&-D_2\exp(-\gamma_{mnz})\}]\cos\alpha_mx\cos\alpha_ny\end{aligned}\quad(16)$$

where the symbol($\wedge$) signifies the Laplace transformatiion, andd m, n denote the sequence of numbers.

2.2 Analysis of impact load considering the local deformation

The analytical model of impact loading for the collision of a ball of mass M with velocity V_o on an infinite plate is shown in Fig. 2.

To simplify the calculation, a circular coordinate is chosen at an ordinary point of impact, and

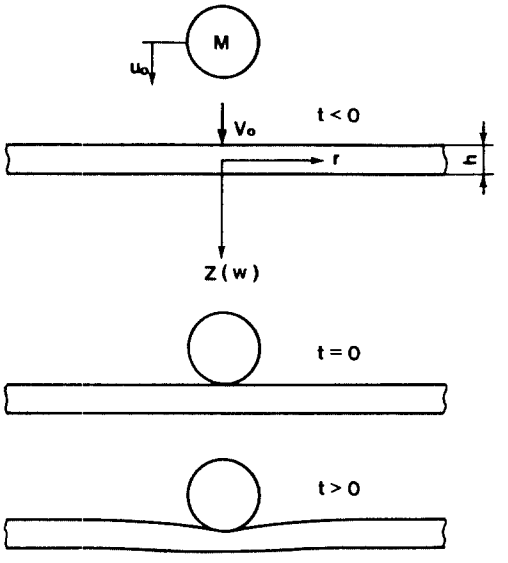

Fig. 2 A model for analyzing impact loading

t(time) at contact moment of ball and plate is to be zero. The magnitude of contact force is F_o, and the function of time variations is $f(t)$.

2.2.1 Displacement of the steel ball

The kinetic equation of the ball is given by

$$M(d^2u_o/dt^2) = -F_o f(t) \tag{17}$$

where u_o is the shifting volume of the ball, M is a mass of steel ball and $F_o f(t)$ is impact loading. The initial condition is as follows when u_o(colliding moment) is zero is as follows:

$$(u_o)_{t=o}=0,\ (du_o/dt)_{t=o}=V_o \tag{18}$$

The solution can be obtained by integrating Eq. (17) with the aid of Eq. (18) as follows:

$$u_o = V_o t - \frac{F_o}{M}\int_o^t\int_o^\xi f(\eta)d\eta d\xi \tag{19}$$

2.2.2 Displacement of the plate

To obtain the displacement of the plate, the Lagrange's kinetic equation of classical plate theory can be used as follows(Timoshenko and Gere , 1961):

$$D\nabla^4 w + \rho h\frac{\partial^2 w}{\partial t^2} = q_o(r,\ t) \tag{20}$$

$$\nabla^2 = \partial^2/\partial r^2 + 1/r \cdot \partial/\partial r,$$

$$D = Eh^3/12(1-\nu^2)$$

where w is the displacement of plate, $q(r,\ t)$ is the uniformly distributed load, E is the elastic modulus, ν is the Poisson's ratio, ρ is the density of plate, and h is the thickness of plate. By using the Laplace transformation and Hankel transformation, one can get

$$\tilde{\bar{w}} = cJ_1(cs)q_o/sp(Ds^4+\rho hp^2) \tag{21}$$

where $\bar{w}=\int_o^\infty we^{-pt}dt$, $\tilde{w}=\int_o^\infty rwJ_o(sr)dr$

Here, the symbol($\sim$) means the Hankel transformation and s is the Hankel transformation parametar.

Substituting the concentrated loading F_o into uniform loading $q_o(q_o\pi c^2 \to F_o,\ J_1(cs)/cs \to 1/2)$, one obtainbs

$$\tilde{\bar{w}} = F_o/2\pi p(Ds^4+\rho hp^2) \tag{22}$$

Again, by using Hankel-inverse transformation and Laplace-inverse transformation at the case $r=0$, one obtains

$$(w)_{r=o} = F_o t/8\sqrt{\rho hD} \tag{23}$$

where r is a radius of plate.

When the load varies with time, the following equation is obtained by the composition-law of Laplace transformation:

$$(w)_{r=o} = (F_o/8\sqrt{\rho hD})\int_o^t f(\xi)d\xi \tag{24}$$

where $u_o-(w)_{r=o}$ is the approach distance of the steel ball and plate.

2.2.3 Nondimensional impact loading

When a ball collides with an infinite plate, the Hertzian contact theory(Goldsmith, 1960) can be appllied to the analysis of the impact loading(Zukas, Theodore, etc., 1976) as follows:

$$u_o-(w)_{r=o} = \{F_o f(t)/k\}^{2/3}$$

$$k = 4\sqrt{r_o}/3(\delta_1+\delta_2)$$

$$\delta_1 = (1-\nu^2)/E$$

$$\delta_o = (1-\nu_o^2)E_o \tag{25}$$

where ν_o is the Possion's ratio of the ball, E_o is the elastic modulus of the ball, and r_o is the radius of the ball.

At the mass point, the kinetic equation is applied to the ball, and Lagrange's kinetic equation of classical plate theory is used on the plate. By substituting Eqs. (19) and (24) into Eq. (25), impact loading is analyzed and the following can be derived(Yang, 1988) in consideration of the deformation of the ball and plate in contact:

$$IP\{p(\tau)\}^{2/3}=\tau-\int_o^\tau\int_o^\xi P(\eta)d\eta d\xi - \int_o^\tau P(\eta)d\eta \qquad (26)$$

where IP denotes the impact loading coefficient as given by

$$IP=\frac{1}{M}\left(\frac{1}{V_o}\right)^{1/3}\left(\frac{1}{k}\right)^{2/3}\left(\frac{8D}{C_b}\right)^{5/3},$$

$$\tau=\frac{8D}{MC_b}t,\ \rho(\tau)=\frac{C_b}{8DV_o}F_o f(t)$$

$$C_b=\sqrt{\frac{Dh}{\rho}}$$

where $p(\tau)$ is the non-dimensional impact loading, M is the mass of steel ball, V_o is the colliding velocity of steel ball, k is the Hertzian contact coefficient, D is the flexural rigid coefficient of plate, and ρ is the density of plate.

2.3 Functional approximation analyses of implusive stresses

Impact loading Eq. (26) cannot be solved analytically due to nonlinear integral equation. If the impact loading can be approximated to the analyzable functions, impulsive stresses can be analyzed. Therefore, in this study, to analyze impulsive stress over ranges of all impact conditions, a new method is proposed in proportion to dimensions of impact loading coefficients.

Impact loading obtained by approximate Eq. (26) with the forward difference method should correspond with the peak of approximate load obtained by the approximate equation proposed, and the initial rising point of the impulsive wave is approximated by the method of least squares as equal as possible. Also, it is proposed that the impulse of two loads should be in accord.

2.3.1 The case where the impact loading parameter, IP, is below 0.2750

In this study within the range of IP 0.03−0.2750 the functional approximate equation of impact loading is suggested by the equation below in order to analyze impulsive stresses at an acting point of impact loading, and it is proposed that impact loading $f(t)$ is working as in Fig. 3(a).

$$f(t)=\begin{cases} At\exp(-\omega t) : 0\le t\le t_o \\ 0 \qquad\qquad\quad t>t_o \end{cases} \qquad (27)$$

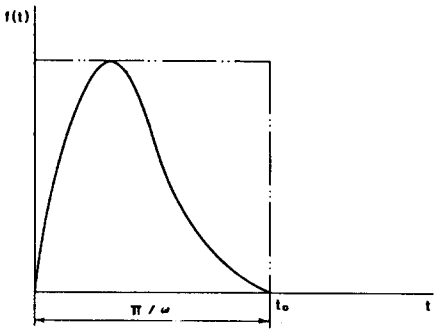

(a) (IP<0.3075)

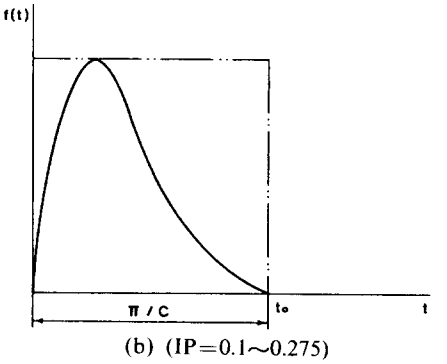

(b) (IP=0.1∼0.275)

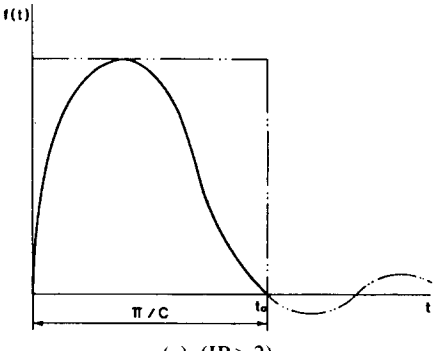

(c) (IP>2)

Fig. 3 Load-time curve

The available range of load, $f(t)$ is as follows:

$$f(t)=At\exp(-\omega t)\cdot U(t) \cdot U(\pi/\omega-t) \qquad (28)$$

Also, to use impulsive stress analysis, the Laplace transformation of Eq. (28) becomes

$$f(p)=\frac{A}{(\omega+p)^2}[1-\exp\{-\pi(1+p/\omega)\}] - \frac{A\pi\exp\{\pi(1+p/\omega)\}}{\omega(\omega+p)} \qquad (29)$$

By substituting Eq. (29) into the Laplace trans-

formation equations of Eq. (11) at upper and lower sides of plate, undetermined coefficients are decided, and by applying with the Laplace inverse transformation, impulsive stresses can be analyzed at an acting point of concentrated impact loading.

Especially in the case of impact problems within the range of IP, 0.1−0.2750, the functional approximate equation of impact loading is suggested as follows:

$$f(t)=\begin{cases} A\exp(-Bt)\{1-\exp(Ct)\} & : 0\le t\le t_o \\ 0 & : t>t_o \end{cases} \tag{30}$$

It is suggested that impact loading $f(t)$ of Eq. (30) is working as shown in Fig. 3(b) within the range of $U(t)\cdot U(\pi/c-t)$. The Laplace transformation of the Eq. (30) becomes

$$\bar{f}(p)=\frac{A}{(cs^2+cs\cdot C)}[C+\{-(cs+C+cs\exp(-C))\}\exp\{-(cs)\pi/c\}] \tag{31}$$

where $cs=p+B$.

2.3.2 The case where the impact loading parameter, IP, is over 0.2750

In the case where IP is over 0.2750, the functional approximate equation of impact loading is as follows:

$$f(t)=\begin{cases} A\exp(-Bt)\sin Ct & : 0\le t\le t_o \\ 0 & : t>t_o \end{cases} \tag{32}$$

This impact loading is working as shown in Fig. 3(c) with the above conditions.

When impact loading, $f(t)$ is working within the range of $U(t)\times U(\pi/c-t)$, application of the Laplace Transformation gives

$$\bar{f}(p)=\frac{AC}{(cs^2+C^2)}[\exp\{(C-cs)\pi/C\}+1] \tag{33}$$

3. Numerical Calculation

In this study, the related equations of strain and stress components in the Laplace transformation region, which are analyzed by the three-dimensional dynamic theory of elasticity in Chapter 2.1, are found by the inverse Laplace transformation, and impulsive stresses are analyzed. But the inverse Laplace transformation is difficult under the three-dimensional dynamic theory of elasticity. Thus, by using F. F. T. such as the equation below(Ujihash, Adachi, Inoue and Matsumoto, 1986), impulsive stresses are analyzed by the numerical inverse Laplace transformation:

$$(\phi_o,\ \lambda_1,\ \lambda_2)_k=\frac{\exp(\gamma\cdot k\Delta t)}{T}\sum_{n=0}^{N-1}(\hat{\phi}_o,\ \hat{\lambda}_1,\ \hat{\lambda}_2)_n\times\exp(i2\pi nk/N)$$
$$(k=0,\ 1,\ 2,\ \cdots,\ N-1) \tag{34}$$

where $(\phi_o,\ \lambda_1,\ \lambda_2)_k=(\phi_o,\ \lambda_1,\ \lambda_2)_{t=k}\cdot\Delta_t$, $(\phi_o,\ \lambda_1,\ \lambda_2)_n=(\phi_o,\ \lambda_1,\ \lambda_2)_{p=r+tn\Delta\omega}$ and $i=\sqrt{-1}$. γ is the real part and ω is the imaginary part of the Laplace transformation parameter, N is number and T is time of the sample subdivision, and $t=T/N$, $\Delta\omega=2\pi/T$ and $\gamma>0$. Also, to improve precision of calculation it is proposed that the nondimensional length is x/h, and the nondimensional time is $(c_1/h)t$. On applying numerical calculation, a variable, γ of Eq. (34) is used as $6/T$(Krings and Waller, 1979).

4. Experimental Apparatus and Method

4.1 Experimental apparatus

In this experiment, to shoot with required velocity, a horizontal-air-pressure impact testing apparatus(manufactured by V. TEK Corp.), whose schematic diagram is shown in Fig. 4(b) was used. Also, Fig. 4 (a) shows a low velocity impact testing apparatus utilized in this research. By using an electromagnetic holder, a steel ball can be made to fall by using a switch.

4.2 Experimental method

Glasses used in this experiment are square plates 300 mm long on each side. Bi-axial strain gauges adhere to the center of the glass plate, and when measured strain ε_x is equal to ε_y by impacting on the opposite side, it is assumed that a ball collides on the center of a square plate.

Specimens are simply supported, strain is measured within the range before the glass plate breaks. Also, material constants using numerical calculation are obtained by the three point bend-

(a)

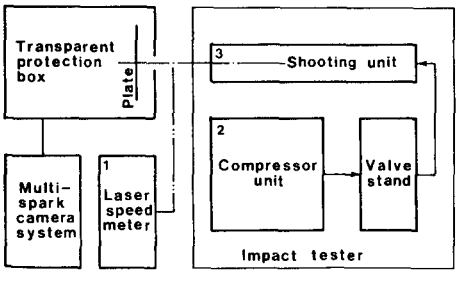

(b)

1. V. TEK Helium-neon Laser
2. V. TEK(Pressure : 10 kg/cm^2)
3. V. TEK(V_{max}=100 m/sec)

Fig. 4 (a) Horizontal type impact testing apparatus (b) The schmatic diagram of horizontal type impact testing apparatus(manufactured by V. TEK. Corp)

ing test, which shows that the longitudinal elastic modulus, E is 67.6 Gpa and the Poisson's ratio ν is 0.22.

5. Comparison of Experimental Results and Theoretical Solutions

In this chapter, to give credit to the analytical methods of implusive stesses which use the three-dimensional dynamic theory of elasticity and functional approximate equation of impact loading proposed in this study, the calculated results of the numerical inverse Laplace transformation of strain Eq. (27) are compared with the results of the measuring strain at an acting point of concentrated impact loading.

5.1 The case where the impact loading parameter, IP, is below 0.2750

As in the case of Fig. 5 where a steel ball 15

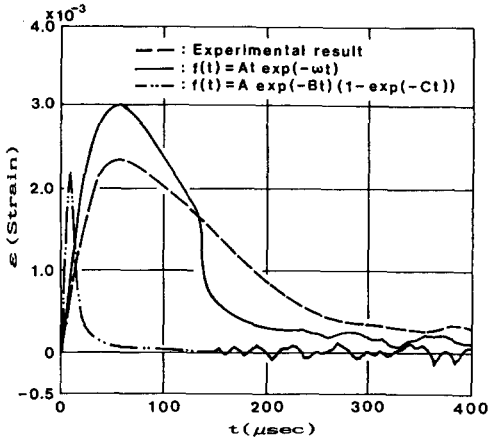

Fig. 5 Comparision of analytical solutions with experimental results of variation with time of strain at an impact point(r_o=7.5 mm, h=2 mm, v_o=4.5 m/sec, IP=0.0398)

mm in diameter with a velocity of 4.5 m/sec impacts on a plate 2 mm thick, Fig. 6 shows how a steel ball 20 mm in diameter with a velocity of 7 m/sec impacts on a plate 5 mm thick, and experimental and numerical calculated results of strain are compared.

At Figs. 5 and 6, solid lines show numerically calculated solutions obtained by using $f(t)=At\exp(-\omega t)$, the functional approximate equation of impact loading, which is newly proposed in this study, one-dotted chain lines indicate $f(t)=A\exp(-Bt)\sin Ct$ and two-dotted chain lines $f(t)=A\exp(-Bt)(1-\exp(-Ct))$. Dotted lines show measurements of experimental results of strain.

Also, in the case of IP=0.0398, the approximate equation($f(t)=A\exp(-Bt)\sin Ct$) cannot be applied, and for the time with the application of the approximate equation $f(t)=At\exp(-\omega t)$, the errors(about 12.5%) occur between strain peak value(3.017×10^{-3}) and experimental results (2.64×10^{-3}); also time(56.25 μsec, 52 μ sec) from 0 to peak points is approximate to that of expermental results.

Therefore, in the case of IP=0.0398 it was found that the functional approximate equation, $f(t)=At\exp(-\omega t)$, was appropriate.

In the case of IP=0.2750, Fig. 6 shows that all

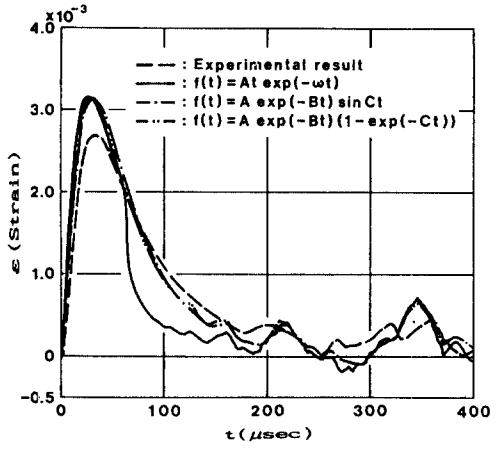

Fig. 6 Comparision of analytical solutions with experimental results of variation with time of strain at an impact point(r_0=10 mm, h=5 mm, v_0=7 m/sec, IP=0.2750)

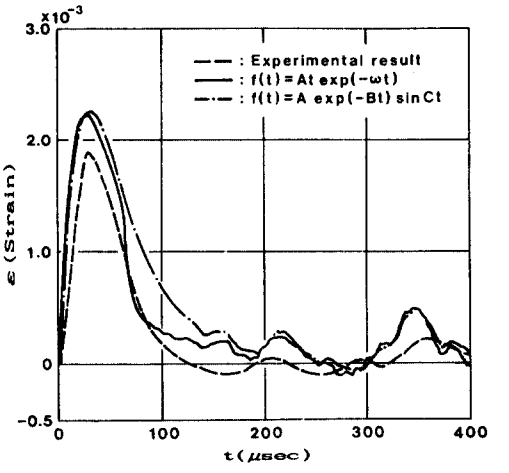

Fig. 7 Comparision of analytical solutions with experimental results of variation with time of strain at an impact point(r_0=10 mm, h=5 mm, v_0=5 m/sec, IP=0.3075)

peak points are almost approximate to 3.15×10^{-3} when the above three approximate equations are used, and the errors(approximately 15%) occur as the measuring strain value(2.7×10^{-3}) is compared with theoretical analytical results. Therefore, it was found that the above three approximate equations were all applicable to this experimentation.

However, there is a slight difference between analytical and experimental results ; firstly, experimental results appear lower than analytical solutions due to the average value of various points corresponding to any area of the strain gauges in the experiments contrary to the value of one point in analyses, and secondly, because the steel ball cannot fall at an exact point on the opposite side of the gauges which adhered to the plate in the experiment, anaytical solutions are considerably larger than experimental results. Thus it is thought that our methods come to an almost agreement with the practical phenomena given the above errors.

5.2 The case where the impact loading parameter, *IP*, is over 0.2750

As in the case of Fig. 7 which shows a steel ball 20 mm in diameter with a velocity of 5 m/sec impacts on a plate 5 mm thick, Fig. 8 shows how a steel ball 5 mm in diameter with a velocity of 70 m/sec impacts on a plate 3 mm thick, and numeri-

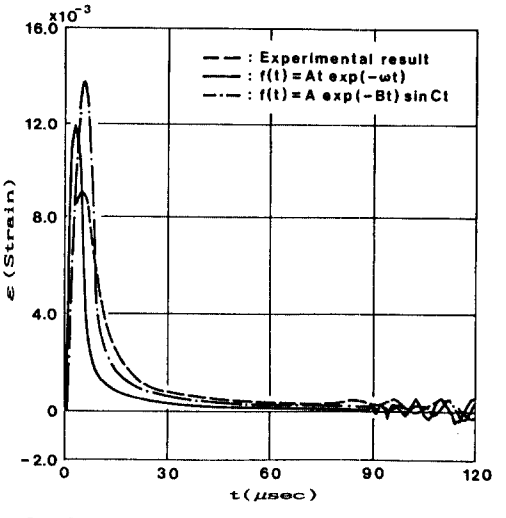

Fig. 8 Comparision of analytical solutions with experimental results of variation with time of strain at an impact point(r_0=2.5 mm, h=3 mm, v_0=70 m/sec, IP=2.3613)

cal calculated and experimental results are compared.

In comparing the application of $f(t)=At\exp(-\omega t)$ with that of $f(t)=A\exp(-Bt)\sin Ct$ on *IP*, 0.3075, as shown in Fig. 7, errors of approximately 0.6%(difference of peak points of strain 2.212×10^{-3} and 2.2256×10^{-3}) occur, and the errors(approximately 14%) occur at 1.8×10^{-3}

peak points of measuring strain. Also, the time on the peak points of strain waves appears at 28.12 μ sec, 31.24 μsec, 28 μsec in that order, and in the case of $f(t)=A\exp(-Bt)\sin Ct$ it shows that errors of appoximately 10%, difference to practical phenomena at peak points formed. Thus, in the case of $IP=0.3075$, the two approximate equations above are both applied ; it shows that $f(t)=A\exp(-\omega t)$ is more appropriate.

In the case of $IP=2.3613$ by using approxmiate equations $f(t)=A\exp(-\omega t)$ and $f(t)=A\exp(-Bt)\sin Ct$ strain peak points of numerical calculated solutions are 1.192×10^{-3} and 1.368×10^{-3} in each and the difference of the two is approximately 14%. When compared with the expermental results, the error of the former is 34.5% and that of the latter is 25%. When compared with only strain peak point, it has been found that the approximate equation of the latter is more approximate. And when compared with time(3.12 μsec, 5.47 μsec) from the ordinary point to peak points it has been found that the former is more approximate.

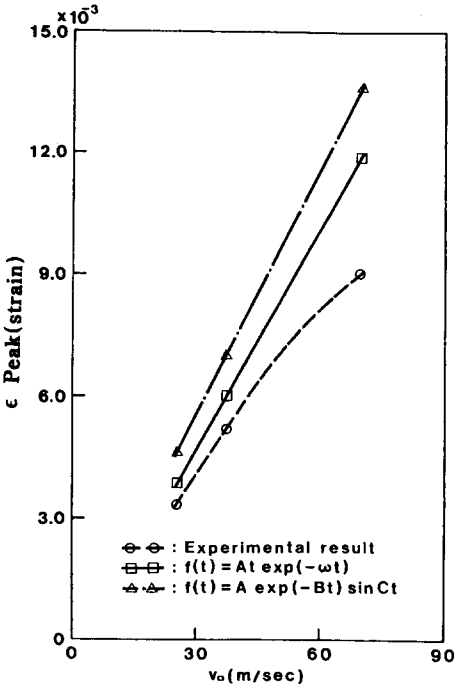

Fig. 9 Variation of max. strain by the impact velocity(r_0=2.5 mm, h=3 mm)

Therefore in the case where IP is over 0.3075, by multiplying $f(t)=A\exp(-Bt)\sin Ct$ by the compensatory factor 0.85 it has been found that the approximate equation is approximate to the practical phenomena. When a steel ball 5 mm in diameter with a velocity of 25 m/sec, 40 m/sec, and 70 m/sec impacts on a plate 5 mm thick, Fig. 9 exhibits the results of numerical calculation and measured strain along the impact velocity. Namely, in a high-velocity case as shown in Fig. 9 and in the case where the dimension of the steel ball sphere and thinkness of the plate are constant, experimental results obtained lower than analytical solutions because instrumental response could not be determined as colliding velocity became faster ; and it was thought that the values of the impact load are overestimated in comparison to practical phenomena.

Therefore, considering the above reason, it is thought that errors between analytical and experimaental results are approximate. In the case where IP is over 0.3075, to analyze impulsive stresses, this approximate equation can be recommened : $f(t)=0.85A\exp(-Bt)\sin Ct$, which is multiplied by the compensative factor 0.85.

6. Conclusions

The functional approximation equation of impact loading should be reformulated for the purpose of analyzing impulsive stresses at an acting point of concentrated impact load of plate under any impact conditions.

The results obtained from this study are as follows :

(1) Impulsive stresses cannot be analyzed directly under an acting point of concentrated impact loading in classical plate theory of plate, but can be successfully analyzed by using the 3-dimensional dynamic theory of elasticity.

(2) The functional approximation equation of impact loading, newly proposed as $f(t)=At\exp(-\omega t)$, seems to be most approximate to the case when IP is below 0.3075,

(3) The functional approximation equation of impact loading, $f(t)=0.85A\exp(-Bt)\sin Ct$, seems to be most approximate to the case when

IP is over 2

(4) Within the *IP* range of 0.2−0.2750, it is noted that the three functional approximation equations of impact loading, $f(t)=At\exp(-\omega t)$, $f(t)=A\exp(-Bt)$, and $f(t)=A\exp(-Bt)\{1-\exp(-Ct)\}$, can all be applied. The larger IP is the more quickly the peak time appears compared with that of practical phenomena.

Acknowledgements

The authors would like to thank Mr. Jong-Ho Kim and Mr. Taek-Hyun Jang for their assistance for the preparation of experimental data.

References

Achenbach, J. D., 1975, Wave Propagation in Elastic Solids, North-Holland Publishing Co., New York, p. 67.

Goldsmith, W., 1960, Impact, Edward Arnold, London, p. 83.

Holian Kathleen S., 1990, "Hydrondynamics Code Calculating of Debris Clouds Produced by Ball-Plate Impacts," Int. J. Impact Engng., Vol. 10, pp. 231~239.

Johnson, W., 1972, Impact Strength of Materials, Edward Arnold, London p. 106.

Kishimoto, K., Aoki, S. and Sakata, M., 1980, "Simple Formula for Dynamic Stress Intensity Factor of Precracked Charpy Specimen," Engng. Fract. Mech., Vol. 13, p. 501.

Krings, W. and Waller, H., 1979, "Contribution to the Numerical Treatment of Partial differential Equations with the Laplace Transformation-An Application of the Algorithm of the Fast Laplace Transformation," Int. J. Num. Method Enging. Vol.14, p. 1186.

Nakahara, I., 1977, Theory of Applied Elasticity, Jitsu-Kyu Publishing Co., Tokyo, p. 207.

Ni Hei-Shu , 1985, Theory of Morden Elasticity, OMU Publishing Co., Tokyo, pp. 26~34.

Timoshenko, S. P. and Gere, J. M., 1961 "Theory of Elastic Stability," McGraw-Hill Co.,New York, pp. 1~370.

Timoshenko, S. P. and Winowsky, K. S., 1959, Theory of Plates and Shells, McGraw-Hill Co., New York, p. 69.

Ugural, A. C., 1981, Stress in Plate and Shells, McGraw-Hill Co., New York, p. 38.

Ujihashi, S. Y., Adachi, T. H., Inoue, H. T. and Matsumoto, H. Y., 1986, "An Analytical and Experimental Study of Impulsive Stresses in a Glass plate Subjected to the Transverse Impact of Steel Balls," JSME(A), Vol. 52, No. 474, pp. 505~531.

Ujihashi, S. Y., 1983, "Impact Response Analysis of Beam by High-Order Approximate Equation," JSME(A), Vol. 49, No. 448, pp. 152~153.

Wang Xiaowei and Yew Ching H., 1989, "Hypervelocity Impact of Two Spheres," Int. J. Impact Engng., Vol. 8, No. 3, pp. 229~240.

Yang, I. Y., 1988, "An Analytical Study of Impulsive Stresses in a Square Plate Subjected to a Concentrated Impact using the Three-Dimensional Dynamic Theory of Elasticity," Chonnam National University.

Zukas, J. A., Theodore Nicholas, etc., 1976, "Impact Dynamic," John Wiley & Sons, New York, p. 57.